An Automated Hirschberg Test for Infants

Dmitri Model*, *Student Member, IEEE*, and Moshe Eizenman

***Abstract*—A novel automated method to measure eye misalignment in infants is presented. The method uses estimates of the Hirschberg ratio (HR) and angle Kappa (the angle between the visual and optical axis) for each infant to calculate the angle of eye misalignment. The HR and angle Kappa are estimated automatically from measurements of the direction of the optical axis and the coordinates of the center of the entrance pupil and corneal reflexes in each eye when infants look at a set of images that are presented sequentially on a computer monitor. The HR is determined by the slope of the line that describes the direction of the optical axis as a function of the distance between the center of the entrance pupil and the corneal reflexes. The peak of the distribution of possible angles Kappa during the image presentation determines the value of angle Kappa. Experiments with five infants showed that the 95% limits of agreement between repeated measurements of angle Kappa are $\pm 0.61^\circ$. The maximum error in the estimation of eye alignment in orthotropic infants was 0.9° with 95% limits of agreement between repeated measurements of 0.75°.**

***Index Terms*—Angle kappa, Eye tracking, Hirschberg ratio (HR), Hirschberg test (HT), optical axis, strabismus, visual axis.**

I. Introduction

THE Hirschberg test (HT) to measure binocular ocular misalignment was introduced more than 120 years ago [1]. It is still being used as the primary clinical method to measure ocular misalignment prior to strabismus surgery in patients for which the alternate prism and cover test cannot be used reliably (i.e., infants and young children). The test is performed by estimating/measuring the displacement of the virtual image of a light source, which is created by the front surface of the cornea (corneal reflex), from the center of the entrance pupil, when subjects fixate on the light source. During the test, the displacement in one eye (the fixating eye or the nondeviating eye in patients with strabismus) is estimated first and the displacement in the other eye is adjusted [2]. The adjustment compensates for angle Kappa of the deviating eye under the assumption that angles Kappa of the two eyes exhibit mirror symmetry [2]. Ocular misalignment is calculated by multiplying the adjusted displacement of the deviating eye by a proportionality constant known as the Hirschberg ratio (HR) [2]. The HR represents the amount of horizontal ocular rotation (in degrees) per millimeter of horizontal displacement of the corneal reflex from the center of the entrance pupil.

The mean value of the HR is approximately 12.5°/mm with an intersubject variability of more than $\pm 20\%$ of the mean value [3]–[6]. Angle kappa may have both horizontal and vertical components of up to $\pm 5^\circ$ [7]. Both angle Kappa and the HR are subject-dependent and have to be estimated for each subject to achieve accurate measurements of eye misalignment. This paper describes a novel automated HT (AHT) that uses estimates of the HR and angle Kappa to calculate eye misalignment.

In contrast to earlier methods to automatically measure eye misalignment [3], [4], [8]–[10], the AHT allows free head movements and does not assume accurate fixation on any specific target, and is therefore, more suitable for use with infants.

The paper is organized as follows. The novel AHT is described in Section II. Experiments with infants are described in Section III. The discussion and conclusions are presented in Section IV.

II. Automated Hirschberg Test

The AHT is based on measurements from a remote two-camera gaze-estimation system that does not require a user-calibration procedure [11]. The system calculates the position and orientation of each eye in space using the coordinates of the pupil centers and corneal reflexes (see Fig. 1, inset). The pupil centers and corneal reflexes are detected and tracked automatically in pairs of images (see Fig. 1) that are captured simultaneously by an eye-tracking system.

In the following analysis, all points are represented as 3-D column vectors (bold font) in a right-handed Cartesian world coordinate system (WCS). The origin of the WCS is at the center of a computer screen that is positioned in front of the subject (Fig. 2, inset). The X_w-axis is horizontal, the Y_w-axis is vertical pointing up, and the Z_w-axis perpendicular to the screen, pointing out of the screen. The analysis is based on the model that is described in Fig. 2, in which the light sources are modeled as point sources, the video cameras are modeled as pinhole cameras and the front surface of the cornea is modeled as a spherical section. The line connecting the center of curvature of the cornea **c**, and the pupil center **p**, defines the optical axis of the eye. Only one of the M ($M \geq 2$) light sources of the system is shown in the Figure.

A. Estimation of the Optical Axis of the Eye

Some of the equations in this section were presented earlier [11]–[14] and they are repeated here for completeness.

Manuscript received May 12, 2010; revised August 10, 2010; accepted September 11, 2010. Date of publication October 7, 2010; date of current version December 17, 2010. . This work was supported in part by a grant from the Natural Sciences and Engineering Research Council of Canada (NSERC), and in part by the scholarships from NSERC and the Vision Science Research Program Award (Toronto Western Research Institute, University Health Network, Toronto, ON, Canada). *Asterisk indicates corresponding author.*

*D. Model is with the Department of Electrical and Computer Engineering, University of Toronto, Toronto, ON M5S 3G4, Canada (e-mail: dmitri.model@utoronto.ca).

M. Eizenman is with the Department of Electrical and Computer Engineering, the Department of Ophthalmology and Vision Sciences, and the Institute of Biomaterials and Biomedical Engineering, University of Toronto, Toronto, ON M5S 3G49, Canada (e-mail: eizenm@ecf.utoronto.ca).

Digital Object Identifier 10.1109/TBME.2010.2085000

Fig. 1. Pair of images of a six-month-old baby obtained during the experiments using a remote binocular gaze-tracking system with two video cameras and three infrared light sources. Pupil center and three corneal reflexes (marked by a cross and squares, respectively) are identified and tracked automatically by the system (see inset).

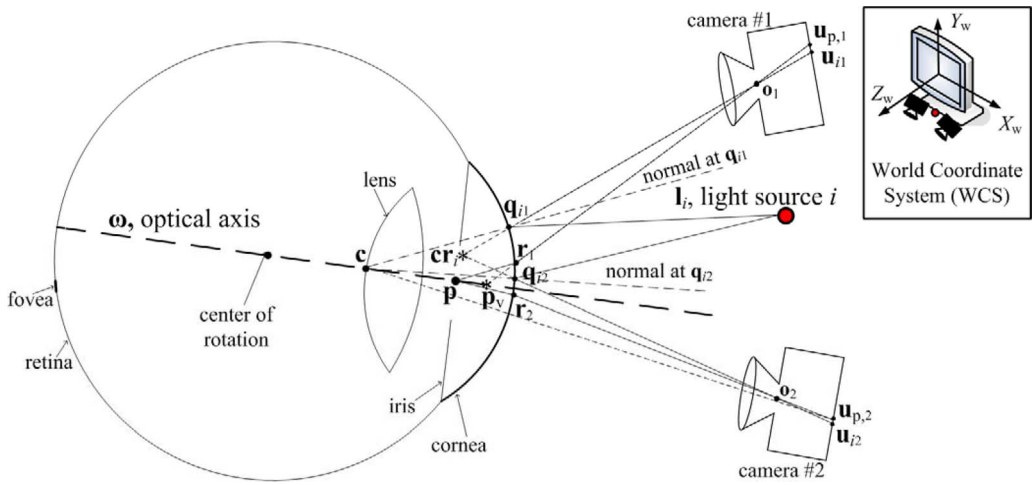

Fig. 2. Ray-tracing diagram (not to scale in order to be able to show all the elements of interest), showing schematic representations of the eye, two cameras and one of the light sources of the system. Inset: remote gaze-estimation system and WCS.

First, consider a ray that originates at a light source i, $\mathbf{l}_i$, travels to a point $\mathbf{q}_{ij}$ on the corneal surface such that the reflected ray goes through the nodal point of camera j, $\mathbf{o}_j$, and intersects the camera image plane at a point $\mathbf{u}_{ij}$. Then, $\mathbf{q}_{ij}$ can be expressed as

$$\mathbf{q}_{ij} = \mathbf{o}_j + k_{q,ij} \frac{\mathbf{o}_j - \mathbf{u}_{ij}}{\|\mathbf{o}_j - \mathbf{u}_{ij}\|} \tag{1}$$

where $k_{q,ij}$ represents the distance between the point of reflection $\mathbf{q}_{ij}$, and the nodal point of the camera $\mathbf{o}_j$.

According to the law of reflection, the incident ray, the reflected ray, and the normal at the point of reflection $\mathbf{n}_{q,ij}$ are coplanar, and the normal at the point of reflection $\mathbf{n}_{q,ij}$ is a bisector of an angle $\mathbf{l}_i - \mathbf{q}_{ij} - \mathbf{o}_j$. Thus

$$\mathbf{n}_{q,ij} = \frac{\mathbf{l}_i - \mathbf{q}_{ij}}{\|\mathbf{l}_i - \mathbf{q}_{ij}\|} + \frac{\mathbf{o}_j - \mathbf{q}_{ij}}{\|\mathbf{o}_j - \mathbf{q}_{ij}\|}. \tag{2}$$

Since any normal to the spherical surface goes through the center of curvature of the cornea $\mathbf{c}$, then

$$\mathbf{c} = \mathbf{q}_{ij} - R \frac{\mathbf{n}_{q,ij}}{\|\mathbf{n}_{q,ij}\|} \tag{3}$$

where R is the radius of the cornea.

Equations (1)–(3) suggest that for each combination of a camera $j = 1, 2$ and a light source $i = 1, \ldots, M$, $\mathbf{c}$ can be expressed as a function of two parameters

$$\mathbf{c}_{ij} = \mathbf{c}_{ij}\left(k_{q,ij}, R\right). \tag{4}$$

Since all the $\mathbf{c}_{ij}$ should be equal to each other, the unknown parameters can be estimated by solving the following minimization problem

$$\underset{i=1,\ldots,M;j=1,2}{\left[\hat{k}_{q,ij}, \hat{R}\right]} = \arg\min \sum_{(i,j)\neq(k,l)} \left\|\mathbf{c}_{ij}\left(k_{q,ij}, R\right) - \mathbf{c}_{kl}\left(k_{q,kl}, R\right)\right\|^2 \tag{5}$$

where the summation is over all possible distinct combinations of $\mathbf{c}_{ij}$ and $\mathbf{c}_{kl}$.

Finally, $\mathbf{c}$ is obtained as an average of all the $\mathbf{c}_{ij}$

$$\mathbf{c} = \frac{1}{N} \sum_{i,j} \mathbf{c}_{ij}(\hat{k}_{q,ij}, \hat{R}) \tag{6}$$

where $N = 2M$ in the case of two cameras and M light sources.

Then, consider an imaginary ray that originates at the pupil center $\mathbf{p}$, travels through the aqueous humor and cornea (effective index of refraction ≈ 1.3375), and refracts at a point $\mathbf{r}_j$ on the corneal surface as it travels into the air (index of refraction ≈ 1) such that the refracted ray passes through the nodal point of camera j, $\mathbf{o}_j$, and intersects the camera image plane at a point $\mathbf{u}_{p,j}$. This refraction results in the formation of an image of the center of the entrance pupil $\mathbf{p}_{v,j}$ located on the extension of the refracted ray, i.e.,

$$\mathbf{p}_{v,j} = \mathbf{o}_j + k_{p,j} \underbrace{(\mathbf{o}_j - \mathbf{u}_{p,j})}_{\mathbf{h}_j}, \qquad \text{for some } k_{p,j}\,. \tag{7}$$

In strict terms, the spatial location of $\mathbf{p}_{v,j}$ depends on the position of the nodal point of the camera $\mathbf{o}_j$ relative to the eye. Therefore, in general, the spatial location of $\mathbf{p}_{v,j}$ will be slightly different for each of the two cameras. Despite this, an approximate center of the entrance pupil $\mathbf{p}_v$ can be found as the midpoint of the shortest segment defined by a point belonging to each of the lines given by (7), $j = 1, 2$, i.e.,

$$\mathbf{p}_v = \frac{1}{2}\begin{bmatrix}\mathbf{h}_1 & \mathbf{h}_2\end{bmatrix}\begin{bmatrix}\mathbf{h}_1\cdot\mathbf{h}_1 & -\mathbf{h}_1\cdot\mathbf{h}_2\\ -\mathbf{h}_1\cdot\mathbf{h}_2 & \mathbf{h}_2\cdot\mathbf{h}_2\end{bmatrix}^{-1} \cdot \begin{bmatrix}-\mathbf{h}_1\cdot(\mathbf{o}_1-\mathbf{o}_2)\\ \mathbf{h}_2\cdot(\mathbf{o}_1-\mathbf{o}_2)\end{bmatrix} + \frac{1}{2}(\mathbf{o}_1+\mathbf{o}_2). \tag{8}$$

Since $\mathbf{c}$ is on the optical axis of the eye and assuming that $\mathbf{p}_v$ is also on the optical axis (see Fig. 2), the optical axis of the eye in 3-D space can be reconstructed using (1)–(8) without the knowledge of any subject-specific eye parameters. The direction of the optical axis of the eye is given by the unit vector

$$\boldsymbol{\omega} = \frac{\mathbf{p}_v - \mathbf{c}}{\|\mathbf{p}_v - \mathbf{c}\|}. \tag{9}$$

The horizontal component of the direction of the optical axis θ can be calculated as the angle between $\boldsymbol{\omega}$ and the plane $X_w = 0$, which is given by

$$\theta = \sin^{-1}(\boldsymbol{\omega}\cdot\hat{\mathbf{x}}) \tag{10}$$

where $\hat{\mathbf{x}}$ is a unit vector in the direction of X_w-axis of the WCS.

Similarly, the vertical component of the direction of the optical axis φ can be calculated as the angle between $\boldsymbol{\omega}$ and the plane $Y_w = 0$, which is given by

$$\varphi = \sin^{-1}(\boldsymbol{\omega}\cdot\hat{\mathbf{y}}) \tag{11}$$

where $\hat{\mathbf{y}}$ is a unit vector in the direction of Y_w-axis of the WCS.

B. Displacement of the Corneal Reflex From the Center of the Entrance Pupil

The position of the virtual image of each light source $\mathbf{l}_i$ (corneal reflex), $\mathbf{cr}_i$, is estimated as the intersection of the rays defined by the nodal point of the camera $\mathbf{o}_j$ and the position of the center of the image of the corneal reflex in the image plane of that camera $\mathbf{u}_{ij}$

$$\mathbf{cr}_{ij} = \mathbf{o}_j + k_{i,j}\underbrace{(\mathbf{o}_j - \mathbf{u}_{ij})}_{\mathbf{a}_j} \qquad \text{for some } k_{i,j}, j = 1, 2. \tag{12}$$

In strict terms, the spatial location of $\mathbf{cr}_{ij}$ depends on the position of the nodal point of the camera $\mathbf{o}_j$ relative to the eye. Therefore, in general, the spatial location of $\mathbf{cr}_{ij}$ will be slightly different for each of the two cameras. Despite this, an approximate virtual image of the light source $\mathbf{cr}_i$ can be found as the midpoint of the shortest segment defined by a point belonging to each of the lines given by (12), $j = 1, 2$, i.e.,

$$\mathbf{cr}_i = \frac{1}{2}\begin{bmatrix}\mathbf{a}_1 & \mathbf{a}_2\end{bmatrix}\begin{bmatrix}\mathbf{a}_1\cdot\mathbf{a}_1 & -\mathbf{a}_1\cdot\mathbf{a}_2\\ -\mathbf{a}_1\cdot\mathbf{a}_2 & \mathbf{a}_2\cdot\mathbf{a}_2\end{bmatrix}^{-1} \cdot \begin{bmatrix}-\mathbf{a}_1\cdot(\mathbf{o}_1-\mathbf{o}_2)\\ \mathbf{a}_2\cdot(\mathbf{o}_1-\mathbf{o}_2)\end{bmatrix} + \frac{1}{2}(\mathbf{o}_1+\mathbf{o}_2). \tag{13}$$

Since the position of the center of the entrance pupil is already calculated in (8), the horizontal displacement of the corneal reflex from the center of the entrance pupil is given by

$$\Delta x = (\mathbf{cr}_i - \mathbf{p}_v)\cdot\hat{\mathbf{x}} \tag{14}$$

where $\hat{\mathbf{x}}$ is a unit vector in the direction of X_w-axis of the WCS.

Similarly, the vertical displacement of the corneal reflex from the center of the entrance pupil is given by

$$\Delta y = (\mathbf{cr}_i - \mathbf{p}_v)\cdot\hat{\mathbf{y}} \tag{15}$$

where $\hat{\mathbf{y}}$ is a unit vector in the direction of Y_w-axis of the WCS.

C. Calculation of the HR

The HR represents the amount of ocular rotation per millimeter of the displacement of the corneal reflex from the center of the entrance pupil. Due to the spherical symmetry of the eye around the optical axis, the HR in the vertical direction is the same as the HR in the horizontal direction. In the following discussion, we describe the estimation of the HR in the horizontal direction. The estimated HR, however, can be used for the calculations of eye misalignment in both the horizontal and vertical directions.

The method to automatically estimate the HR in infants was first described by us in [5]. In this section, we describe the sensitivity of the method to head movements and provide a more complete technical description.

During the estimation procedure, subjects looked naturally at a set of small video images (2 cm $\times$ 2 cm) that were presented sequentially on a computer monitor. The horizontal component of the direction of the optical axis (θ) given by (10), and the horizontal distance between the center of the entrance pupil and the corneal reflex (Δx) given by (14) were calculated. Fig. 3 shows an example of data recorded with a six-month-old infant. The absolute value of the slope of the line that is fitted to the data points $(\Delta x_i, \theta_i)$, $i = 1, \ldots, N$ is an estimate of the HR (°/mm). To remove possible outliers (e.g., measurements with large errors due to blinks) a robust estimator (iteratively reweighted least-squares [15]) was used for the line-fitting procedure.

The aforementioned estimation procedure assumes that for each horizontal angle of the optical axis θ, there is only one unique value of Δx. When the head moves, however, Δx might vary, even when θ is constant. This will affect the accuracy of the estimation of the HR. Since head movements cannot be completely eliminated during the short estimation procedure,

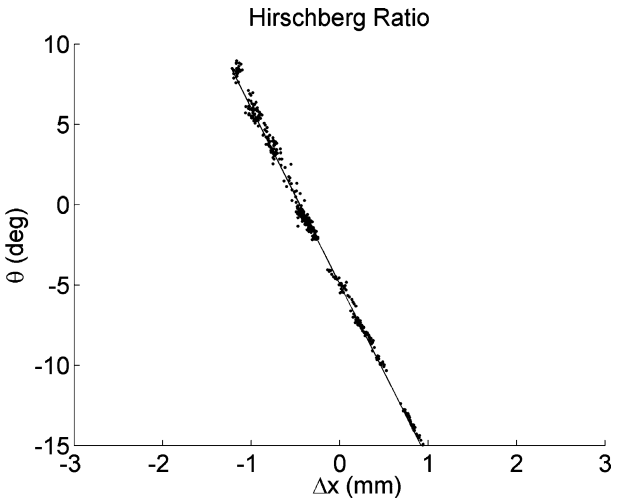

Fig. 3. Horizontal angle of the optical axis (θ) versus the horizontal displacement of the corneal reflex **cr** from the center of the entrance pupil $\mathbf{p}_v$ (Δx). Dots represent data points. The absolute value of the slope of the line that is fitted to the data points represents the HR in °/mm.

especially with infants and young children, it is important to develop algorithms to minimize the effects of head movements on the estimation of the HR.

To develop the algorithm to minimize the effects of head movements, we first used computer simulations to evaluate the effects of head movements on Δx when θ is constant. In the simulations, the head position was changed over a range of ± 100 mm in the X_w, Y_w, and Z_w directions (the approximate allowed range of head movements in the gaze-estimation system used for the experiments) while the direction of the optical axis of the right eye was kept parallel to the Z_w axis ($\boldsymbol{\omega} \| Z_w$). System parameters for the simulations (locations and orientations of the cameras and light sources) were similar to the parameters of the system that was used in the experiments. The initial position of the center of curvature of the simulated right eye of the subject was set at $[0, 0, 750]^T$ mm. For this initial position, the horizontal displacement of the corneal reflex of the middle light source of the system from the center of the entrance pupil is nil ($\Delta x = 0$). The results of the simulations are shown in Fig. 4. Fig. 4(a), shows that for each 10 mm of head movement in the X_w direction, Δx is changed by approximately 0.05 mm. Head movements in the Y_w and Z_w directions have negligible effect on Δx [see Fig. 4(b) and (c)].

Based on the data collected with infants and young children during the estimation of the HR, the expected range of Δx due to eye movements exceeds 1 mm. To ensure that estimation errors due to head movements will not exceed 5% of the actual HR, Δx due to head movements should be limited to less than 5% of the minimum range of Δx due to eye movements (i.e., to 0.05 mm), or equivalently, head movements in the X_w-direction should not exceed 10 mm.

The following algorithm ensures that data used for the calculations of the HR will only correspond to head positions that are within 10 mm of each other along the X_w-axis. The algorithm uses the position of the center of curvature of the cornea of the eye **c** to determine changes in head position. The algorithm has four stages. In the first stage, all data points, (θ_i, Δx_i) $i = 1, \ldots, N$, are partitioned into bins according to the value of the x-component of $\mathbf{c}_i$ and $\mathbf{c}_{i,x}$ (the width of each bin is 10 mm). In the second stage, the bin with the largest number of data points is selected. In the third stage, the average value $\bar{\mathbf{c}}_x$ of all $\mathbf{c}_{i,x}$ in the selected bin and in the two adjacent bins is calculated. In the fourth stage, data points that satisfy the constraint $|\bar{\mathbf{c}}_x - \mathbf{c}_{i,x}| < 5$ mm are used with the line-fitting procedure to calculate the HR.

Fig. 5(a) shows the data points that were collected during the estimation of the HR with a six-month-old infant. The data suggest that during the estimation procedure, the infant changed his head position. As the infant continued to make horizontal eye movements at each head position, data points for each head position tend to be along lines that are parallel to each other. Fig. 5(b) shows the data that were retained for the estimation of the HR after the algorithm to remove head movements' artifacts was used.

D. Estimation of Angle Kappa

As was shown in [11], the horizontal α, and vertical β, components of angle Kappa (the angle between the optical and visual axes) can be estimated, if the subject fixates on a known point in space at a specific time interval. With infants, however, it is impossible to guarantee that this requirement will be satisfied and a different strategy had to be used to estimate angle Kappa. The strategy is based on the assumption that when a small attractive stimulus (animated image with sound) is presented on a black background, there is higher probability that the infant will look at the stimulus than at any other point on the computer screen. When a sequence of such stimuli is presented at different locations on the computer screen, the angles α_i and β_i for each time instant i can be calculated under the assumption that the infant is fixating on the presented stimulus. A histogram of α_i and β_i, $i = 1, \ldots, N$, for a sequence of nine stimuli is shown in Fig. 6. If the subject fixates exclusively on the presented stimuli, similar values of α_i and β_i should be computed for all N measurements (i.e., all α_i or β_i should fall in a single bin of the histogram). If, on the other hand, the subject fixates on points on the computer screen that are uncorrelated with the presented stimuli, the histogram shown in Fig. 6 should resemble a uniform distribution. The histograms of α_i and β_i in Fig. 6 exhibit one dominant peak that corresponds to all the time instances for which the infant looked at the stimuli. Note that in the example shown in Fig. 6, the infant looked at the stimuli for 37% of the time that the stimuli were presented on the screen. For the five infants in this study, the average percentage of time that infants looked at the stimuli was 47% (ranged from 26% to 70%).

Since in this study the stimulus spans 1.5° of the viewing angle, all points in the range of $\pm 1.5°$ from the center of the highest bin were averaged to compute the estimate of α and β. Based on the expected magnitude of α and β [6], the range of α and β in Fig. 6 was limited to $|\alpha_i| < 10$ and $|\beta_i| < 5$, respectively.

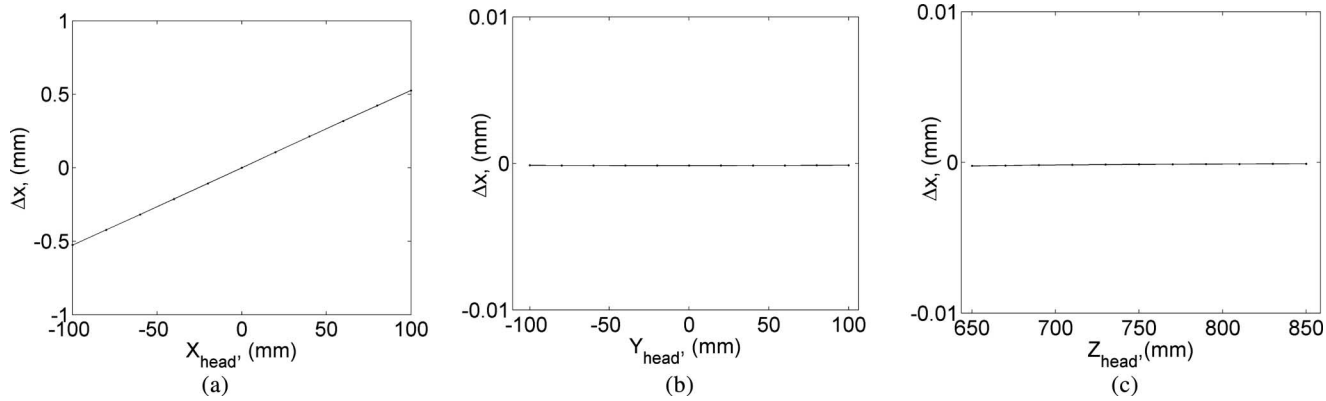

Fig. 4. Effects of head movements on Δx (the horizontal displacement of the corneal reflex from the center of the entrance pupil) when the direction of the optical axis is kept constant. Head movements in the direction of (a) X_w, (b) Y_w, and (c) Z_w.

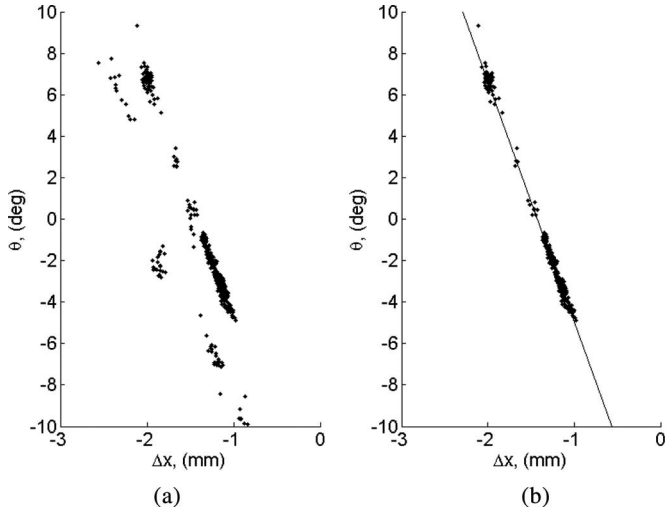

Fig. 5. (a) Data from a six-month-old infant who moved his head during the estimation procedure. (b) Data retained for the estimation of the HR removal of head-movements artifacts. A solid line is fitted to the retained data points. Note that the raw data in (a) can be described by a set of lines that are parallel to the solid line fitted in (b).

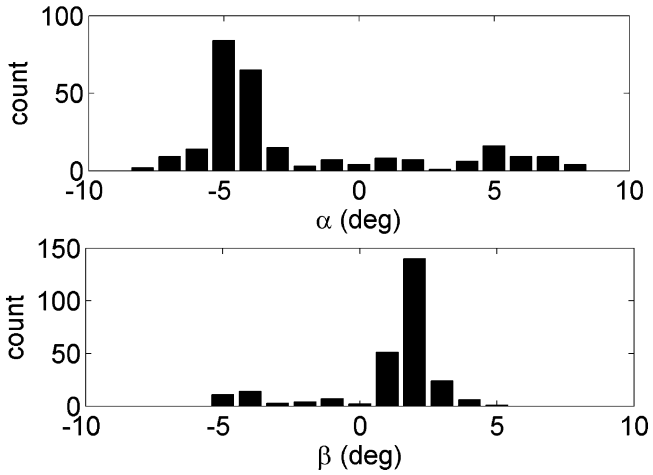

Fig. 6. Histograms of estimated α and β angles for the right eye of eight-month-old infant.

E. Estimation of Eye Misalignment

For each time instant i, the distance from the center of the entrance pupil to the corneal reflex in the left and right eyes Δx_i^L and Δx_i^R, respectively, was calculated using (14). HR was calculated as described in Section II-C. α^L and α^R were calculated as described in Section II-D. Note that α^L should be estimated when the left eye fixates on the stimulus, and α^R should be estimated when the right eye fixates on the stimulus. For patients with strabismus, α^L and α^R should be estimated in two different sessions. Without a loss of generality, let us assume that the right eye is the dominant eye (i.e., the left eye is the deviating eye). In such a case, during binocular viewing, the subject will fixate with the right eye on the stimulus and, hence, only α^R will be estimated. Then, the right eye should be covered to force the subject to fixate with the left eye and the procedure described in Section II-D should be repeated to estimate α^L. If it is not possible to have the right eye patched (e.g., due to low vision in the left eye), $\alpha^L = -\alpha^R$ can be assumed as an approximation [16].

The horizontal angle of eye misalignment is given by

$$\Theta_i = \mathrm{HR}\left(\Delta x_i^L - \Delta x_i^R\right) + \left(\alpha^R - \alpha^L\right). \tag{16}$$

Similarly, the vertical angle of misalignment can be calculated using Δy_i^L and Δy_i^R from (15), and β^L and β^R as follows:

$$\Phi_i = \mathrm{HR}\left(\Delta y_i^L - \Delta y_i^R\right) + \left(\beta^R - \beta^L\right). \tag{17}$$

Finally, histogram-based outlier removal and averaging algorithm similar to the one described in Section II-D is applied to calculate the mean values of Θ and Φ.

III. Experiments

The performance of the AHT was studied with five healthy infants (6-, 8-, 9-, 15-, and 16-month-old). During the experiments, infants were seated on their parents' lap, with their heads supported by the parents' hands. Infants' heads were approximately 85 cm from the computer monitor. The coordinates of the pupil centers and corneal reflexes of the two eyes were obtained by the VISION 2020-RB eye-tracking system (El-MAR Inc., Toronto, ON, Canada). The system has two infrared video cameras and three infrared light sources. The middle light source

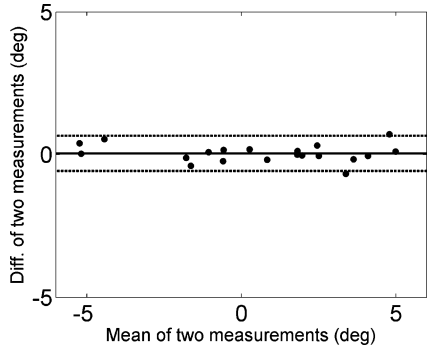

Fig. 7. Difference versus mean plot for two independent measurements of α^L, α^R, β^L, and β^R (five infants). The solid line indicates mean of differences (bias $= 0.04^\circ$). The 95% limits of agreement ($\pm 0.61^\circ$) are indicated by the dashed lines.

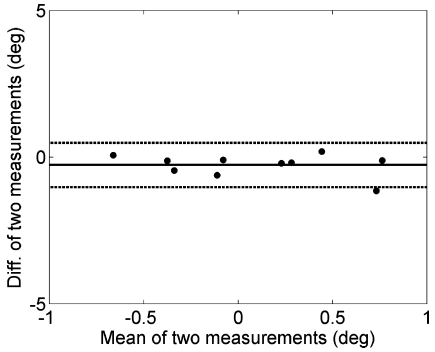

Fig. 8. Difference versus mean plot for two independent measurements of horizontal and vertical angles of eye misalignment (five infants). The solid line indicates mean of differences (bias $= -0.27^\circ$). The 95% limits of agreement ($\pm 0.75^\circ$) are indicated by the dashed lines.

located in the center of the system was used for the estimation of the HR and eye misalignment.

Nine animated images (2 cm $\times$ 2 cm) were presented sequentially at different positions on the monitor and 450 estimates were recorded at a rate of 30 estimates per second. All infants were orthotropic and no eye patching (covering) was necessary for the estimation of angles Kappa in the left and right eyes. The measurement was repeated twice, to assess repeatability [17].

First, we examined the repeatability of estimation of α^L, α^R, β^L, and β^R. The average difference ($\pm$standard deviation, SD) between two independent measurements was $0.04^\circ \pm 0.31^\circ$ and the 95% limits of agreement for repeated measurements were $\pm 0.61^\circ$ (see Fig. 7).

As was shown in [5], the average difference ($\pm$SD) between two measurements of HR were 0.09 $\pm$ 0.32°/mm and the 95% limits of agreement for repeated measurements were ± 0.63 °/mm.

All the measurements of the angles of misalignment Θ and Φ were in a range of -1° to $+1^\circ$. For orthotropic infants, this corresponds to a maximum error of less than 1°. The average difference between two independent measurements of eye misalignment was $-0.27^\circ \pm 0.38^\circ$ and the 95% limits of agreement for repeated measurements were $\pm 0.75^\circ$ (see Fig. 8).

IV. Discussion and Conclusion

A novel AHT procedure to measure accurately eye misalignment in infants and young children was presented. The average difference between two independent measurements of eye misalignment was $-0.27^\circ \pm 0.38^\circ$ and the 95% limits of agreement for repeated measurements were $\pm 0.75^\circ$ (see Fig. 8). The maximum error in the estimation of the horizontal and vertical components of eye misalignment in orthotropic children was less than 1°.

It is important to note that the accuracy of the AHT procedure depends on accurate estimates of the optical axes of the two eyes. These estimates are based on the approximation that the cornea can be modeled as a spherical surface. Significant deviations from this approximation due to corneal pathologies and/or high corneal asymmetry (astigmatism) can affect the accuracy of the measurements, and therefore, the accuracy of the AHT procedure have to be verified with a larger sample of orthotropic and nonorthotropic subjects.

The following example provides insights into the expected errors in the estimation of eye misalignment in infants with strabismus. The example assumes a patient with a 20° infantile esotropia. According to (16) and (17), the estimates of eye misalignment will be affected by errors in the estimates of α^L, α^R, β^L, β^R, and HR. If the maximum errors in these parameters are approximated by the 95% limits of agreement between repeated measurements, the maximum errors in the estimation of α^L, α^R, β^L, and β^R are $\pm 0.61^\circ$ and the maximum error in the HR is ± 0.63 °/mm (5% of the mean value of the HR – 12.5 °/mm). For the aforementioned example, the maximum error in the estimation of Θ due to errors in the estimation of the HR is $20^\circ * 5\% = 1^\circ$ and the maximum error due to errors in the estimation of α^L and α^R is $0.61^\circ * 2 = 1.22^\circ$. The total error in the estimation of Θ is, therefore, less than 2.22°. The example demonstrates that the expected accuracy of the novel AHT with infants is significantly better than the expected accuracy of the standard clinical HT, even when it is performed with cooperative subjects – 5° [18].

The AHT procedure can provide more accurate measurements of ocular misalignment than the standard HT. It may, therefore, enable early and reliable detection of infantile esotropia that may lead to early treatment and increase the chances for normal visual development in these patients [19]–[21].

Acknowledgment

The authors would like to thank Dr. E. Guestrin, Dr. V. Sturm, Dr. A. Wong, and Dr. S. Kraft for their insightful comments.

References

[1] J. Hirschberg, "Ueber messung des schielgrades und dosirung der schieloperation," in *Zentralblatt für Praktische Augenheilkunde*. vol. 8, Leipzig, Germany: Verlag von Veit & Comp., 1885, pp. 325–27.

[2] R. Jones and J. B. Eskridge, "The Hirschberg test: A reevaluation," *Amer. J. Optom.*, vol. 47, no. 2, pp. 105–114, 1970.

[3] J. M. Miller, M. Mellinger, J. Greivenkemp, and K. Simons, "Videographic hirschberg measurement of simulated strabismic deviations," *Invest. Ophthalmol. Vis. Sci.*, vol. 34, no. 11, pp. 3220–3229, Oct. 1993.

[4] S. Hasebe, H. Ohtsuki, Y. Tadokoro, M. Okano, and T. Furuse, "The reliability of a video-enhanced hirschberg test under clinical conditions,"

Invest. Ophthalmol. Vis. Sci., vol. 36, no. 13, pp. 2678–2685, Dec. 1995.
[5] D. Model, M. Eizenman, and V. Sturm N, "Fixation-free assessment of the hirschberg ratio," *Invest. Ophthalmol. Vis. Sci.*, vol. 58, no. 8, pp. 4035–4039, 2010.
[6] F. Schaeffel, "Kappa and hirschberg ratio measured with an automated video gaze tracker," *Optom. Vis. Sci.*, vol. 79, no. 5, pp. 329–334, 2002.
[7] R. H. S. Carpenter, *Movements of the Eyes*. London, U.K.: Pion, 1977.
[8] R. Effert, "A new method for determining squint angle in primary and all secondary positions using the first and fourth Purkinje images," *Ophthalmology*, vol. 93, no. 4, pp. 436–441, 1986.
[9] R. Effert and K. Pflibsen, "A new method to perform the cover test," *Ophthalmology*, vol. 93, no. 4, pp. 433–435, 1986.
[10] D. L. Guyton, A. Moss, and K. Simons, "Automated measurement of strabismic deviations using a remote haploscope and an infrared television-based eye tracker," *Trans. Amer. Ophthalmol. Soc.*, vol. 85, pp. 320–331, 1987.
[11] E. D. Guestrin and M. Eizenman, "Remote point-of-gaze estimation requiring a single-point calibration for applications with infants," in *Proc. 2008 Symp. Eye Tr acking Res Appl.,*, Savannah, GA, 2008, pp. 267–274.
[12] E. D. Guestrin and M. Eizenman, "General theory of remote gaze estimation using the pupil center and corneal reflections," *IEEE Trans. Biomed. Eng.*, vol. 53, no. 6, pp. 1124–1133, Jun. 2006.
[13] D. Model and M. Eizenman, "An automatic personal calibration procedure for advanced gaze estimation systems," *IEEE Trans. Biomed. Eng.*, vol. 57, no. 5, pp. 1031–1039, May 2010.
[14] S. W. Shih and J. Liu, "A novel approach to 3-D gaze tracking using stereo cameras," *IEEE Trans. Syst., Man, Cybern. Part B: Cybern.*, vol. 34, no. 1, pp. 234–245, Feb. 2004.
[15] P. W. Holland and R. E. Welsch, "Robust regression using iteratively reweighted least-squares," in *Communications in Statistics: Theory Methods*, vol. A6, no. 9, 1977, pp. 813–827,.
[16] M. C. Wheeler, "Objective strabismometry in young children," *Arch. Ophthalmol.*, vol. 29, no. 5, pp. 547–564, May 1943.
[17] J. M. Bland and D. G. Altman, "Statistical methods for assessing agreement between two methods of clinical measurement," *The Lancet*, vol. 327, no. 8476, pp. 307–310, 1986.
[18] R. Y. Choi and B. J. Kushner, "The accuracy of experienced strabismologists using the Hirschberg and Krimsky tests," *Ophthalmology*, vol. 105, no. 7, pp. 1301–1306, 1998.
[19] E. M. Helveston, F. D. Ellis, D. A. Plager, and K. K. Miller, "Early surgery for essential infantile esotropia," *J. pediatr. ophthalmol. strabismus,* (discussion 119), vol. 27, no. 3, pp. 115–118, May/Jun. 1990.
[20] G. K. Von Noorden, "A reassessment of infantile esotropia. XLIV edward jackson memorial lecture," *Amer. J. Ophthalmol.*, vol. 105, no. 1, pp. 1–10, 1988.
[21] A. M. Wong, "Timing of surgery for infantile esotropia: Sensory and motor outcomes," *Canadian J. Ophtalmol.*, vol. 43, no. 6, pp. 643–51, 2008.

Dmitri Model (S'90) was born in Moscow, Russia, in 1980. He received the B.Sc. (*cum laude*) and M.Sc. degrees in electrical engineering from Technion-–Israel Institute of Technology, Haifa, Israel, in 2002 and 2006, respectively. He is currently working toward the Ph.D. degree in the Department of Electrical and Computer Engineering, University of Toronto, ON, Canada.

His current research interests include eye tracking and gaze estimation technology and applications, signal and image processing, and numerical optimization.

Moshe Eizenman was born in Tel-Aviv, Israel, in 1952. He received the B.A.Sc., M.A.Sc., and Ph.D. degrees in electrical engineering from the University of Toronto, Toronto, ON, Canada, in 1978, 1980, and1984, respectively.

Since 1984, he has been with the Faculty of the University of Toronto, where he is currently an Associate Professor in the Department of Electrical and Computer Engineering, and the Department of Ophthalmology and Vision Sciences, and also at the Institute of Biomaterials and Biomedical Engineering. He is also a Research Associate at the Eye Research Institute, Canada, and the Hospital for Sick Children, Toronto. His current research interests include detection and estimation of biological phenomena, eye tracking and gaze estimation systems, visual evoked potentials, and the development of vision.